3636 *Chem. Mater.* **1998,** *10,* 3636−3642

Synthesis and Characterization of a New Two-Dimensional Aluminophosphate Layer and Structural Diversity in Anionic Aluminophosphates with $Al_2P_3O_{12}^{3-}$ Stoichiometry

J. Yu,*[†,‡,§] K. Sugiyama,[||] K. Hiraga,[||] N. Togashi,[‡] O. Terasaki,*[†,‡,⊥] Y. Tanaka,[∇]
S. Nakata,[∇] S. Qiu,[§] and R. Xu[§]

CREST, Japan Science and Technology Corporation, Department of Physics, Graduate School of Science, and Center for Interdisciplinary Research, Tohoku University, Sendai 980-8578, Japan, Institute for Materials Research, Tohoku University, Sendai 980-8577, Japan, Key Laboratory of Inorganic Synthesis and Preparative Chemistry, Jilin University, Changchun 130023, People's Republic of China, and R & D Center, Chiyoda Corporation, Yokohama 221-0022, Japan

Received May 28, 1998. Revised Manuscript Received July 23, 1998

A new two-dimensional aluminophosphate layer $[Al_2P_3O_{10}(OH)_2][C_6NH_8]$ (compound **1**) has been prepared from an alcoholic system using 4-methylpyridine (C_6NH_7) as a template. The as-synthesized product is characterized by powder X-ray diffraction, dynamic thermogravimetric, and ^{31}P-, ^{27}Al-, and ^{13}C magic-angle spinning (MAS) NMR analyses. The structure has been solved by single-crystal X-ray diffraction analysis. Compound **1** crystallized in the monoclinic space group $P2_1/c$ (no. 14), with $a = 8.686$ (3) Å, $b = 21.240$ (3) Å, $c = 8.799$ (2) Å, $\beta = 113.23$ (3)°, and $Z = 4$. The inorganic layers are constructed from alternating aluminum units (AlO_4 and AlO_5) and phosphorus units [PO_4, $PO_3(OH)$, $PO_2(=O)(OH)$] and are featured by rows of edge-sharing bridged six-membered rings (6MRs) and zigzag four rings (4MRs). The layers are held with each other through strong H-bondings between the terminal oxygens attached to the 2-connected phosphate groups in adjacent layers. The organic ammonium cations ($C_6NH_8^+$) are located in the large cavities between the interlayer regions. The structural features and relationships in the anionic aluminophosphates with $Al_2P_3O_{12}^{3-}$ stoichiometry, including compound **1** and previously reported compounds, are discussed. Furthermore, new two-dimensional (2-D) networks have been proposed on the basis of the discovered building rules for aluminophosphates with $Al_2P_3O_{12}^{3-}$ stoichiometry.

Introduction

Since 1982, a series of microporous aluminophosphates, $AlPO_4$-*n*, where AlO_4 and PO_4 tetrahedra are alternatively 4-connected through oxygen atoms in the structures, have been hydrothermally synthesized in the presence of various organic templates.[1−5] These materials have potential applications in adsorption and catalysis, like aluminosilicate zeolites. In recent years, by utilizing a nonaqueous synthesis technique,[6] a rich structural and compositional diversity in aluminophosphate (AlPO) families has been achieved. So far, different dimensionalities of AlPO structures have been observed. Except for the class of basic aluminum orthophosphates with the Al/P ratios larger than 1,[7] e.g., trolleite $[Al_4(OH)_3(PO_4)_3]$,[8] augelite $[Al_2(OH)_3(PO_4)]$,[9] and evansite $[Al_3(OH)_6(PO_4)\cdot 6H_2O]$,[10] the stoichiometries of the organically templated AlPOs have been found as $AlPO_4$ ($AlPO_4$-*n*),[1−5,11] $Al_5P_6O_{24}H^{2-}$ (JDF-20, a 3-D AlPO with 20MR openings);[12] $Al_4P_5O_{20}H^{2-}$ (AlPO−HDA, a 3-D AlPO with intersecting 12- and eight-membered channels);[13] $Al_3P_4O_{16}^{3-}$ (a series of 2-D layer materials),[14−24] $Al_2P_3O_{12}^{3-}$ (a series of 2-D layer

---

[†] Japan Science and Technology Corp.
[‡] Department of Physics, Tohoku University.
[§] Jilin University.
[||] Institute for Materials Research, Tohoku University.
[⊥] Center for Interdisciplinary Research, Tohoku University.
[∇] Chiyoda Corp.

(1) Wilson, S. T.; Lok, B. M.; Messian, C. A.; Cannon, T. R.; Flanigen, E. M. *J. Am. Chem. Soc.* **1982**, *104*, 1146.

(2) Flanigen, E. M.; Lok, B. M.; Patton, R. L.; Wilson, S. T. In *New Developments in Catalysis*; Murakami, Y., Ijima, A.; Ward, J. W., Eds.; Elsevier: New York, 1986; p 103.

(3) Bennett, J. M.; Dytrych, W. J.; Pluth, J. J.; Richardson, J. W., Jr.; Smith, J. V. *Zeolites* **1986**, *6*, 349.

(4) Flanigen, E. M.; Patton, R. L.; Wilson, S. T. In *Studies in Surface Science and Catalysis*; Grobet, P. J., Mortier, W. J., Vansant, E. F., Schulz-Ekloff, G., Eds.; Elsevier: New York, 1988; p 13.

(5) Davis, M. E.; Saldarriage, C.; Montes, C.; Garces, J.; Crowder, C. *Nature* **1988**, *331*, 698.

(6) Xu, R.; Huo, Q.; Pang, W. in *Proceedings of the Ninth International Zeolite Conference*; Ballmoos, R. V., Higgins, J. B., Treacy, M. M. J., Eds.; Butterworth-Heinemann: Montreal, 1992; p 271.

(7) Kniep, R. *Angew. Chem., Int. Ed. Engl.* **1986**, *25*, 525.

(8) Moore, P. B.; Araki, T. *Am. Mineral.* **1974**, *59*, 974.

(9) Araki, T.; Finney, J. J.; Zoltai, T. *Am. Mineral.* **1968**, *53*, 1069.

(10) Melon, J.; Touissant, J. *Ann. Soc. Geol. Belg. Bull.* **1957**, *80*, B497.

(11) Meier, W. M.; Olson, D. H.; Baerlocher, Ch. *Atlas of Zeolite Structure Types*; *Zeolites* **1996**, *17*. 1.

(12) (a) Huo, Q.; Xu, R.; Li, S.; Ma, Z.; Thomas, J. M.; Jones, R. H.; Chippindale, A. M. *J. Chem. Soc., Chem. Commun.* **1992**, 875. (b) Jones, R. H.; Thomas, J. M.; Chen, J.; Xu, R.; Huo, Q.; Li, S.; Ma, Z.; Chippindale, A. M. *J. Solid State Chem.* **1993**, *102*, 204.

10.1021/cm980379c CCC: $15.00

compounds),[25−27] $Al_3P_5O_{20}H^{5-}$ (UT-2, 1-D chain),[27] $AlP_2O_8^{3-}$ (a series of 2-D layers[24,28,29] and 1-D chains[30−33]), and $AlP_4O_{16}^{9-}$ (an isolated AlPO cluster).[34] The decrease of the Al/P ratio from 1/1 indicates the tendency of the structural dimensionality deviated from 3-D constructed from fully connected Al and P units, due to the presence of triply, or doubly, or singly bridging phosphate tetrahedra containing terminal oxygen atoms. It has been noted that these phosphate groups with terminal oxygens have potential for self-assembly and further condensation to build up high-dimensional framework.[35] A good example is that the 1-D aluminophosphate chain UT-2 can be thermally transformed to the 2-D layer structure of UT-3.[27] Through further synthesis of new materials and better understanding of the structural features of these aluminophosphate materials, it will assist in reaching a rational design and synthesis of microporous materials with specifically tailored properties.

It has been found that there are four unique structural connectivities for the anionic aluminophosphate layer compounds with $Al_2P_3O_{12}^{3-}$ stoichiometry.[25−27] Herein, we report a new 2-D aluminophosphate $[Al_2P_3O_{10}(OH)_2][C_6NH_8]$ with unique structural architecture and discuss the structural diversity in aluminophosphates including both known and hypothetical 2-D networks with $Al_2P_3O_{12}^{3-}$ stoichiometry.

Experimental Section

Synthesis. All chemicals were purchased from Aldrich. Pure large single crystals of compound **1** are prepared in a gel system with molar composition 1.0 $Al(^iPrO)_3$:(2.4−4.1) H_3PO_4:5 4-methylpyridine:19 2-BuOH at 160−180 °C for 9−12 days. Typically, 2.0 g of finely ground aluminum triisopropoxide was first dispersed into 16 mL of 2-butanol solvent with stirring, followed by addition of 4.8 mL of 4-methylpyridine. Phosphoric acid (85 wt %; 2.72 mL) was finally added dropwise to the above reaction mixture with stirring. A sticky gel was formed and transferred into a 23 mL Parr digestion bomb and heated at 160 °C for 12 days under autogenous pressure. The product was filtered and washed thoroughly with ethanol and deionized water and dried at 70 °C.

Characterization. Powder X-ray diffraction (XRD) patterns were recorded in step scanning ($\Delta 2\theta = 0.02$, step time 10 s) on a Philips PW3050 X-ray diffractometer by using CuKα radiation ($\lambda = 1.5418$ Å) with a graphite monochromator in the diffracted beam path.

Dynamic thermogravimetric (DyTG) analysis was performed on a Rigaku Thermoplus 2 TG 8120 analyzer under He flow with a heating rate of 5 °C/min. The temperature was automatically kept constant while some major weight loss occurred.

Solid-state NMR experiments were performed with magic-angle spinning (MAS) on a Jeol JNM-A-400WB spectrometer operating at frequencies of 100.52, 104.17, and 161.83 MHz for ^{13}C, ^{27}Al, and ^{31}P, respectively. Chemical shifts were referenced to an external standard of tetramethylsilane (TMS) for ^{13}C, $Al(H_2O)_6^{3+}$ for ^{27}Al, and 85% H_3PO_4 for ^{31}P. The sample was spun at 10 kHz for ^{27}Al and at 5.2 kHz for ^{13}C and ^{31}P. Pulse widths were 5.0, 2.0, and 6.0 μs, all recycle delay times were 5.0 s, and totals of 12 000, 160, and 80 scans were taken for ^{13}C, ^{27}Al, and ^{31}P, respectively.

Single-Crystal X-ray Diffraction Structure Analysis. A colorless platelike crystal with dimensions of 0.31 × 0.14 × 0.02 mm was selected and mounted on a thin glass fiber by using cyanoacrylate. The intensity data were collected on a Rigaku AFC7R diffractometer using monochromatic MoKα radiation generated by a rotating-anode X-ray tube. The lattice constants were determined by the least-squares procedure applied to 25 2θ values between 24° and 33°. Intensity data of 4615 reflections ($0 < h < 12$, $0 < k < 29$, $-12 < l < 12$) were collected in the ω-scan mode up to $(\sin \theta/\lambda)_{max} = 0.704$, among which 2772 reflections meet the condition of $I > 2\sigma(I_{obs})$. Measured data were corrected for Lorentz and polarization effects together with an absorption correction by an integration method, ACACA, using an isometric grid.[36] The structure was solved by the direct method SIR92[37] and refined by the least-squares program SHELXL97.[38] During the isotropic refinement of the framework atoms and the non-hydrogen atoms of 4-methylpyridine template molecule, the hydroxylation of O(2) and O(9) and the protonation of the 4-methylpyridine molecule are suggested so as to achieve the charge balance of the present compound. After introduction of anisotropic temperature factors for the framework atoms, possible H(2) and H(9) sites of hydroxyl components were confirmed by difference Fourier maps at a distance of about 0.92 Å near O(2) and O(9), respectively. This prompted us to refine the positions of H(2) and H(9) by using a common riding model with a fixed interatomic distance of O−H = 0.92 Å. Finally, all framework positions were refined anisotropically and then H atoms of protonated 4-methylpyridine were placed geometrically. The isotropic temperature factors for all H-

---

(13) (a) Yu, J.; Sugiyama, K.; Zheng, S.; Qiu, S.; Chen, J.; Xu, R.; Sakamoto, Y.; Terasaki, O.; Hiraga, K.; Light, M.; Hursthouse, M. B.; Thomas, J. M. *Chem. Mater.* **1998**, *10*, 1208. (b) Yu, J.; Sugiyama, K.; Togashi, N.; Zheng, S.; Qiu, S.; Chen, J.; Xu, R.; Sakamoto, Y.; Terasaki, O.; Hiraga, K.; Tanaka, Y.; Nakata, S.; Light, M.; Hursthouse, M. B.; Thomas, J. M. In *Proceedings of the 12th International Zeolite Conference*, in press.

(14) Jones, R. H.; Thomas, J. M.; Cheetham, A. K.; Powell, A. V. *J. Chem. Soc., Chem. Commun.* **1991**, 1266.

(15) Thomas, J. M.; Jones, R. H.; Xu, R.; Chen, J.; Chippindale, A. M.; Natarajan, S.; Cheetham, A. K. *J. Chem. Soc., Chem. Commun.* **1992**, 929.

(16) Chippindale, A. M.; Natarajan, S.; Thomas, J. M.; Jones, R. H. *J. Solid State Chem.* **1994**, *111*, 18.

(17) Jones, R. H.; Chippindale, A. M.; Natarajan, S.; Thomas, J. M. *J. Chem. Soc., Chem. Commun.* **1994**, 565.

(18) Kuperman, A.; Nadimi, S.; Oliver, S.; Ozin, G. A.; Garces, J. M.; Olken, M. M. *Nature* **1993**, *365*, 239.

(19) Morgan, K.; Gainsford, G.; Milestone, N. *J. Chem. Soc., Chem. Commun.* **1995**, 425.

(20) Barrett, P. A.; Jones, R. H. *J. Chem. Soc., Chem. Commun.* **1995**, 1979.

(21) Williams, I. D.; Gao, Q.; Chen, J.; Ngai, L.-Y.; Lin, Z.; Xu, R. *Chem. Commun.* **1996**, 1781.

(22) Oliver, S.; Kuperman, A.; Lough, A.; Ozin, G. A. *Inorg. Chem.* **1996**, *35*, 6373.

(23) Gao, Q.; Li, B.; Chen, J.; Li, S.; Xu, R. *J. Solid State Chem.* **1997**, *129*, 37.

(24) (a) Yu, J.; Williams, I. D. *J. Solid State Chem.* **1998**, *136*, 141. (b) Yu, J.; Williams, I. D.; Qiu, S.; Terasaki, O.; Xu, R. *Supramol. Sci.* **1998**, in press.

(25) Chippindale, A. M.; Powell, A. V.; Bull, L. M.; Jones, R. H.; Cheetham, A. K.; Thomas, J. M.; Xu, R. *J. Solid State Chem.* **1992**, *96*, 199.

(26) Oliver, S.; Kuperman, A.; Lough, A.; Ozin, G. A. *Chem. Commun.* **1996**, 1761.

(27) Oliver, S.; Kuperman, A.; Lough, A.; Ozin, G. A. *Chem. Mater.* **1996**, *8*, 2391.

(28) Morgan, K. R.; Gainsford, G. J.; Milestone, N. B. *Chem. Commun.* **1997**, 61.

(29) Leech, M. A.; Cowley, A. R.; Prout, K.; Chippindale, A. M. *Chem. Mater.* **1998**, *10*, 451.

(30) Jones, R. H.; Thomas, J. M.; Xu, R.; Huo, Q.; Xu, Y.; Cheetham, A. K.; Bieber, D. *J. Chem. Soc., Chem. Commun.* **1990**, 1170.

(31) Wang, T.; Yu, L.; Pang, W. *J. Solid State Chem.* **1990**, *89*, 392.

(32) Chippindale, A. M.; Turner, C. *J. Solid State Chem.* **1997**, *128*, 318.

(33) Williams, I. D.; Yu, J.; Gao, Q.; Chen, J.; Xu, R. *Chem. Commun.* **1997**, 1273.

(34) Riou, D.; Loiseau, T.; FÇrey, G. *J. Solid State Chem.* **1992**, *99*, 414.

(35) Oliver, S.; Kuperman, A.; Ozin, G. A. *Angew. Chem., Int. Ed.* **1998**, *37*, 46.

(36) Wuensch, B. J.; Prewitt, C. T. *Z. Krist.* **1965**, *122*, 24.

(37) Altomare A.; Cascarano, G.; Giacovazzo, G.; Guagliardi, A.; Burla, M. C.; Polidori, G.; Camalli, M. *J. Appl. Cryst.* **1994**, *27*, 435.

(38) Sheldrick, G. M.; SHELXL97, Program for the Refinement of Crystal Structures, University of Gîttingen, Germany, 1997.

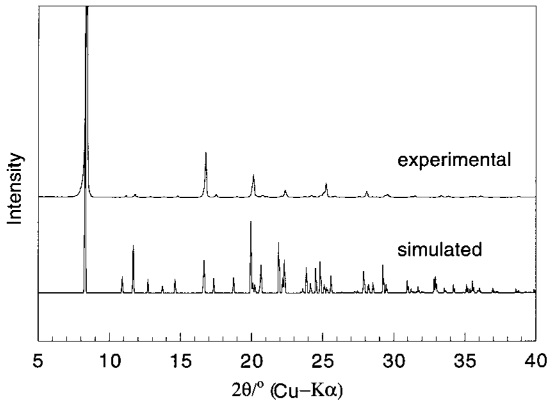

Figure 1. Experimental and simulated powder X-ray diffraction patterns of compound **1**.

Table 1. Crystal Data and Structure Refinement for $Al_2P_3O_{10}(OH)_2C_6NH_8$

empirical formula	$C_6H_{10}Al_2NO_{12}P_3$	
formula weight	435.02	
temperature	298(2) K	
wavelength	0.71069 Å	
crystal system	monoclinic	
space group	$P2_1/c$	
unit cell dimensions	$a = 8.686(3)$ Å	$\alpha = 90°$
	$b = 21.240(3)$ Å	$\beta = 113.23(3)°$
	$c = 8.799(2)$ Å	$\gamma = 90°$
volume	1491.8(6) $Å^3$	
Z	4	
density (calculated)	1.937 Mg/m^3	
absorption coefficient	0.583 mm^{-1}	
$F(000)$	880	
crystal size	0.31 × 0.14 × 0.02 mm	
θ range for data collection	2.55−30.00°	
index ranges	$0 \le h \le 12, 0 \le k \le 29, -12 \le l \le 11$	
reflections collected	4615	
independent reflections	4343 [R(int) = 0.0556]	
absorption correction	integration	
max and min transmission	0.9918 and 0.9300	
refinement method	full-matrix least-squares on F^2	
data/restraints/parameters	4343/2/190	
goodness-of-fit on F^2	1.023	
final R indices [$I > 2\sigma(I)$]	$R_1 = 0.0534$, $_wR_2 = 0.1164$	
R indices (all data)	$R_1 = 0.1269$, $_wR_2 = 0.1357$	
largest diff. peak and hole	0.868 and −0.893 e·$Å^{-3}$	

atoms are constrained to be identical. A summary of selected crystallographic data is given in Table 1.

Results and Discussion

Synthesis and Characterization of Compound 1. Compound **1** formed in the solvothermal system contains large single crystals with a thin platelike shape. The experimental powder XRD pattern and the simulated XRD pattern of compound **1** based on single-crystal X-ray diffraction analysis are shown in Figure 1. Their peak positions are in agreement with each other, suggesting the phase purity of the as-synthesized compound. The differences in intensity may be explained by a preferred orientation effect on the observed XRD pattern.

Dynamic thermogravimetric analysis shows a major weight loss occurring at 162 °C and then gradual weight loss with temperature, as shown in Figure 2. The total weight loss of ca. 28.05% from 160 to 600 °C is in agreement with the calculated amount of 27.6% (21.4% for the decomposition of the template, 6.2% for dehydration of 1.5 moles of H_2O based on the empirical formula).

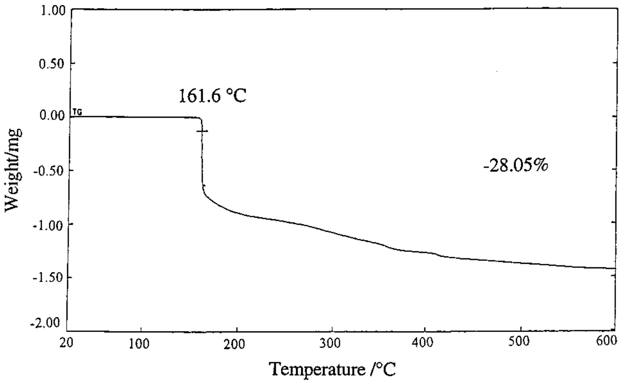

Figure 2. Dynamic thermogravimetric curve of compound **1**.

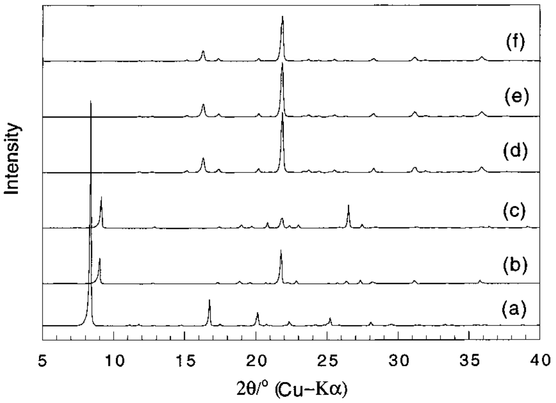

Figure 3. X-ray diffraction patterns of samples as synthesized (a) and calcined at (b) 180, (c) 250, (d) 350, (e) 500, and (f) 700 °C.

The samples calcined in air at different temperatures were studied by powder XRD analysis as shown in Figure 3. Compound **1** changes its structure at 180 and 250 °C (Figure 3b,c), and their peak positions could be indexed by a triclinic phase. Above 350 °C, the reflections from the known dense phases, berlinite (JCPDS card no. 10-0423) and $AlPO_4$ (JCPDS card no. 11-0500) become dominant. Further investigation of the structural change upon heating together with compositional change is underway.

Single-crystal XRD analysis indicates that compound **1** crystallizes in the monoclinic $P2_1/c$ (no. 14). Table 2 shows the final atomic coordinates and isotropic temperature factors for compound **1**. Selected bond lengths and bond angles are listed in Table 3.

The structure of compound **1** contains macroanionic sheets $Al_2P_3O_{10}(OH)_2^-$ that are charge-balanced by the protonated 4-methylpyridine ($C_6NH_8^+$). The asymmetric unit contains two crystallographically distinct Al sites, tetrahedral $Al(1)O_4$ and distorted trigonal bipyramide $Al(2)O_5$. ^{27}Al MAS NMR spectrum (Figure 4a) shows two signals at 40.3 and 12.7 ppm, corresponding to AlO_4 and AlO_5, respectively.[39] The Al(1)−O bond lengths are in the range 1.718−1.746 Å and the O−Al(1)−O angles are in the range 106.6∼113.0°, which are typical for aluminophosphate materials. The two axial Al(2)−O distances are 1.908 and 1.872 Å, while the three shorter Al(2)−O distances are in the range 1.777−

---

(39) Stöcker, M. Advanced Zeolite Science and Applications. In *Studies in Surface Science and Catalysis*; Jansen, J. C., Stöcker, M., Karge, H. G., Weitkamp, J., Eds.; Elsevier: New York, 1994; Vol. 85, p 429.

Table 2. Atomic Coordinates (× 10^4) and Equivalent Isotropic Displacement Parameters (Å^2 × 10^3) for $Al_2P_3O_{10}(OH)_2C_6NH_8$[a]

	x	*y*	*z*	*U*(equiv)/iso
P(1)	9557(1)	964(1)	−713(1)	11(1)
P(2)	4584(1)	2504(1)	−595(1)	11(1)
P(3)	9859(1)	1968(1)	3207(1)	11(1)
Al(1)	6971(1)	2072(1)	−2192(1)	11(1)
Al(2)	1937(1)	2089(1)	873(1)	11(1)
O(1)	9227(4)	652(1)	671(3)	18(1)
O(2)	9674(4)	445(1)	−1930(3)	19(1)
O(3)	8092(3)	1378(1)	−1790(3)	21(1)
O(4)	1175(3)	1344(1)	−112(3)	18(1)
O(5)	5417(3)	2028(1)	−4189(3)	16(1)
O(6)	3490(3)	2033(1)	−166(3)	15(1)
O(7)	5946(3)	2115(1)	−853(3)	16(1)
O(8)	3606(3)	2122(1)	2857(3)	17(1)
O(9)	9647(4)	1246(1)	3365(3)	21(1)
O(10)	283(3)	2104(1)	1737(3)	18(1)
O(11)	1195(3)	2824(1)	−147(3)	16(1)
O(12)	8198(3)	2725(1)	−2020(3)	19(1)
C(1)	3990(6)	−148(2)	−3328(6)	34(1)
C(2)	5292(6)	90(2)	−1947(6)	35(1)
C(3)	5065(6)	638(2)	−1215(6)	31(1)
N(1)	3596(5)	937(2)	−1870(5)	31(1)
C(4)	2353(6)	740(2)	−3239(6)	34(1)
C(5)	2519(7)	192(3)	−3981(7)	37(1)
C(6)	4167(8)	−763(3)	−4087(8)	59(2)
H(1)	10130(8)	71(16)	−1440(7)	73(7)
H(2)	9410(8)	1030(3)	2400(4)	73(7)
H(3)	6315	−119	−1516	73(7)
H(4)	5924	796	−278	73(7)
H(5)	3449	1270	−1387	73(7)
H(6)	1371	974	−3693	73(7)
H(7)	1640	49	−4925	73(7)
H(8)	3631	−1090	−3722	73(7)
H(9)	5334	−861	−3753	73(7)
H(10)	3650	−730	−5270	73(7)

[a] *U*(equiv) is defined as one-third of the trace of the orthogonalized $\mathbf{U}_{ij}$ tensor.

Table 3. Selected Bond Lengths and Angles for $Al_2P_3O_{10}(OH)_2C_6NH_8$

Bond Lengths (Å)			
P(1)−O(1)	1.510 (3)	Al(1)−O(7)	1.737 (3)
P(1)−O(4)^b	1.524 (3)	Al(1)−O(5)	1.746 (3)
P(1)−O(3)	1.530 (3)	Al(2)−O(8)	1.777 (3)
P(1)−O(2)	1.567 (3)	Al(2)−O(11)	1.789 (3)
P(2)−O(8)^c	1.516 (3)	Al(2)−O(4)	1.800 (3)
P(2)−O(6)	1.527 (3)	Al(2)−O(10)	1.872 (3)
P(2)−O(5)^d	1.528 (3)	Al(2)−O(6)	1.908 (3)
P(2)−O(7)	1.532 (3)	C(1)−C(5)	1.380 (7)
P(3)−O(10)^b	1.506 (3)	C(1)−C(2)	1.388 (7)
P(3)−O(11)^e	1.521 (3)	C(1)−C(6)	1.501 (8)
P(3)−O(12)^d	1.523 (3)	C(2)−C(3)	1.381 (7)
P(3)−O(9)	1.558 (3)	N(1)−C(4)	1.329 (6)
Al(1)−O(12)	1.718 (3)	C(4)−C(5)	1.371 (7)
Al(1)−O(3)	1.726 (3)		
Bond Angles (deg)			
O(1)−P(1)−O(4)^b	113.28 (16)	O(8)−Al(2)−O(4)	120.63 (14)
O(1)−P(1)−O(3)	112.10 (16)	O(11)−Al(2)−O(4)	122.28 (14)
O(4)^b−P(1)−O(3)	109.75 (16)	O(8)−Al(2)−O(10)	93.42 (13)
O(1)−P(1)−O(2)	109.09 (16)	O(11)−Al(2)−O(10)	90.42 (13)
O(4)^b−P(1)−O(2)	108.07 (16)	O(4)−Al(2)−O(10)	90.88 (13)
O(3)−P(1)−O(2)	104.07 (16)	O(8)−Al(2)−O(6)	90.92 (13)
O(8)^c−P(2)−O(6)	112.53 (15)	O(11)−Al(2)−O(6)	89.80 (12)
O(8)^c−P(2)−O(5)^d	107.80 (15)	O(4)−Al(2)−O(6)	84.80 (12)
O(6)−P(2)−O(5)^d	111.59 (15)	O(10)−Al(2)−O(6)	175.02 (13)
O(8)^c−P(2)−O(7)	110.02 (15)	P(1)−O(3)−Al(1)	152.0 (2)
O(6)−P(2)−O(7)	105.95 (15)	P(1)^g−O(4)−Al(2)	138.30 (18)
O(5)^d−P(2)−O(7)	108.92 (15)	P(2)^c−O(5)−Al(1)	135.35 (17)
O(10)^b−P(3)−O(11)^e	114.13 (15)	P(2)−O(6)−Al(2)	134.77 (17)
O(10)^b−P(3)−O(12)^d	110.20 (15)	P(2)−O(7)−Al(1)	139.52 (18)
O(11)^e−P(3)−O(12)^d	109.11 (15)	P(2)^d−O(8)−Al(2)	148.70 (19)
O(10)^b−P(3)−O(9)	110.05 (16)	P(3)^g−O(10)−Al(2)	146.36 (18)
O(11)^e−P(3)−O(9)	105.92 (16)	P(3)^h−O(11)−Al(2)	136.07 (18)
O(12)^d−P(3)−O(9)	107.12 (17)	P(3)^c−O(12)−Al(1)	151.6 (2)
O(12)−Al(1)−O(3)	113.02 (15)	C(5)−C(1)−C(2)	118.3 (5)
O(12)−Al(1)−O(7)	111.41 (14)	C(5)−C(1)−C(6)	120.7 (5)
O(3)−Al(1)−O(7)	107.71 (14)	C(2)−C(1)−C(6)	119.9 (5)
O(12)−Al(1)−O(5)	109.77 (13)	N(1)−C(3)−C(2)	119.2 (5)
O(3)−Al(1)−O(5)	108.03 (14)	C(4)−N(1)−C(3)	122.5 (4)
O(7)−Al(1)−O(5)	106.63 (13)	N(1)−C(4)−C(5)	119.9 (5)
O(8)−Al(2)−O(11)	116.87 (14)	C(4)−C(5)−C(1)	120.0 (5)

[a] Symmetry transformations used to generate equivalent atoms are as follows: ^{b} $x + 1, y, z$. ^{c} $x, -y + {}^1/_2, z - {}^1/_2$. ^{d} $x, -y + {}^1/_2, z + {}^1/_2$. ^{e} $x + 1, -y + {}^1/_2, z + {}^1/_2$. ^{f} $-x + 2, -y, -z$. ^{g} $x - 1, y, z$. ^{h} $x - 1, -y + {}^1/_2, z - {}^1/_2$.

1.800 Å. Of the three crystallographically distinct P sites, P(2) shares four oxygens with adjacent Al atoms with P−O distances varying between 1.516 and 1.532 Å. P(3) has one hydroxyl group, characterized by the longer bond distance P(3)−O(9) of 1.558 Å. The H atom associated with O(9) is found in the difference Fourier map. P(1) only shares two oxygens with adjacent Al(1) and Al(2) units, leaving two oxygens terminal. The P(1)−O(2) bond has a longer distance of 1.567 Å and an H atom is found associated with O(2), while the shortest bond distance P(1)−O(1) of 1.510 Å suggests double-bonding character.[15] The ^{31}P cross-polarization (CP) MAS NMR spectrum (Figure 4b) shows three peaks at −10, −19.6, and −20.4 ppm, which might be assigned to the three distinct P sites $PO_2({=}O)(OH)$, $PO_3(OH)$, and PO_4, respectively.[39,40] The inorganic sheet of compound **1** is constructed from alternating these Al units including AlO_4, and AlO_5 and P units including PO_4, $PO_3(OH)$, and $PO_2(OH)({=}O)$.

Figure 5 shows the inorganic network of compound **1** along the *b* direction. The structure is characterized by a series of edge-sharing 6MRs and zigzag 4MRs arranged in alternative rows. The 2-connected phosphate groups $P(1)O_2({=}O)(OH)$ exclusively bridge the six-membered rings alternatively above and below the sheet, which forms rows of bridged-6MR.

The inorganic sheets are further held together through strong H-bondings between the terminal O atoms attached to P(1) tetrahedra protruding into the interlayer region (Figure 6), characterized by an O···O distance between O(2) and O(1) from the adjacent layer of 2.594 (4) Å and an O(2)−H···O(1) angle of 173.9 (6.5)°. Strong H-bondings are also found to exist between O(1) and O(9) within the layer, with a P(1)O(1)···H−O(9)−P(3) separation of 2.580 (4) Å and an O(1)···H−O(9) angle of 150.0 (4.7)°. Large cavities are formed between the two layers, in which the organic templates reside. ^{13}C CP MAS NMR analysis gives four peaks appearing at 24.1, 126.6, 145.6, and 163.9 ppm, in agreement with the four nonequivalent carbon sites in 4-methylpyridine ^{1}CH3^{3}C^{2}CH^{4}CHN^{4}CH^{2}CH. This suggests that the template molecules are intact in the structure. It is noted that the aromatic planar template molecules are aligned antiparallel with each other (Figure 6). The organic cation, acting as a space-filler and a charge-balancer for the anionic inorganic framework, also serves as H-bonding donor to the nearest framework oxygen O(6), characterized by an N−H···O(6)−P(2) separation of

---

(40) Nakayama, H.; Eguchi, T.; Nakamura, N.; Yamaguchi, S.; Danjyo, M.; Tsuhako, M. *J. Mater. Chem.* **1997**, *7*, 1063.

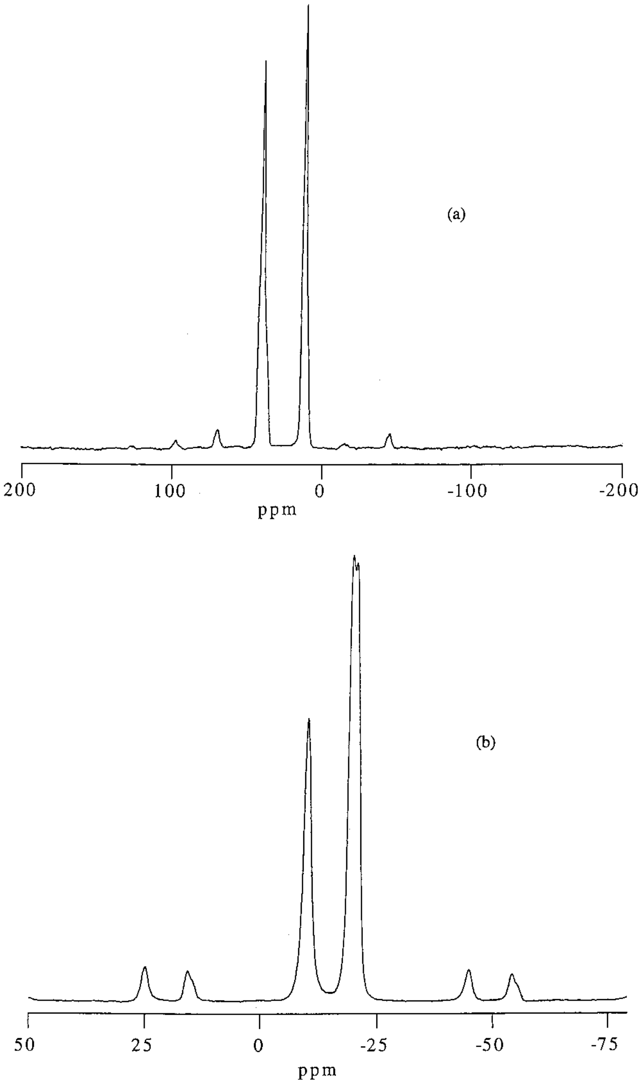

Figure 4. MAS NMR spectra of compound **1**: (a) ^{27}Al-MAS NMR; (b) ^{31}P CP MAS NMR.

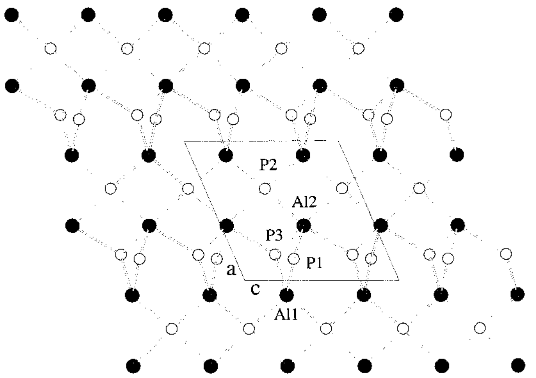

Figure 5. Sheet structure of compound **1** viewed along the *b* direction (oxygen atoms are omitted).

2.790 (5) Å and N–H···O(6) angle of 171.2°. It can be seen that the inorganic structure is subtly controlled by the organic templates.

Interestingly, in compound **1** the existence of terminal phosphate groups $P(1)O_2(=O)(OH)$ implies some potentials for further condensation to build up high-dimensional material (Figure 6). Ideally, the structure of compound **1** can be set up for condensation of additional Al units across the P(1)–O(1)···HO(2)–P(1) hydrogen bonding bridges to form Al6P6 12MR channels along the *c* direction.

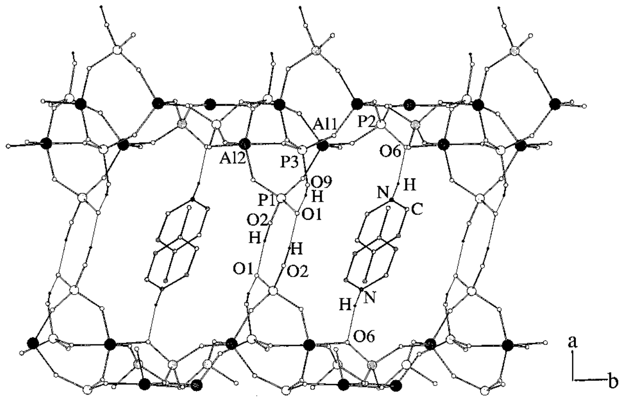

Figure 6. Structure of compound **1** viewed along the *c* direction (hydrogen bonds are indicated by fine lines).

Structural Diversity in Anionic Aluminophosphates with $Al_2P_3O_{12}^{3-}$ Stoichiometry. The empirical formula of $[Al_2P_3O_{12}H_x]^{x-3}\cdot(3-x)R^+$ ($x = 1, 2$; R = organic amine) has been found in the previously reported five 2-D aluminophosphate compounds, of which four are unique in structures.[25-27] The geometries of the five unique structures, including compound **1**; compound **2**, $Al_2P_3O_{12}H_2\cdot PyH$;[25] compound **3**: $Al_2P_3O_{12}H\cdot 2C_5NH_{12}$ (UT-5);[26] compound **4**, $Al_2P_3O_{12}H\cdot 2C_5NH_{12}$ (UT-4);[26] and compound **5**, $Al_2P_3O_{12}H\cdot 2BuNH_3$,[25] are shematically shown in Figure 7. The black and white circles indicate the up and down features of triply bridging phosphate groups.

Compounds **1** and **2** have common basic building units including AlO_4 and AlO_5 and phosphorus groups with 4-, 3-, and 2-connected oxygens. However, the former is characterized by a series of edge-sharing bridged-6MR as discussed above (Figure 7, structure 1), while the latter is featured by intergrown capped-6MRs in which triply, bridging phosphate groups cap the six-rings alternatively up and down. The intergrown capped-6MRs are connected with each other through 4MRs that form an 8MR (Figure 7, structure 2).

The other three compounds **3**, **4**, and **5** contain the same basic building units, i.e., tetrahedral AlO_4 and triply, doubly bridging tetrahedral phosphate units with terminal =O and –OH/=O groups. Their structures are characterized by a series of rows of edge-sharing bridged-6MR, as the case in compound **1**. In compound **3**, rows of bridged-6MR sharing edges along one direction are connected, forming 6MRs (Figure 7, structure 3), whereas in compounds **4** and **5**, rows of bridged-6MR sharing edges in a zigzag arrangement are connected to form 4- and 8MRs (Figure 7, structure 4) and 6MRs (Figure 7, structure 5), respectively. The rows of edge-sharing bridged-6MR can be rotated 180° along the line perpendicular to the row in the plane for forming a 2-D net, and they are indicated by the arrows for clarity.

It is noted that through breaking the bonding between the pentacoordinated Al and four-connected tetrahedral phosphorus, the structure of compound **1** can be exactly converted to that of compound **3**.

On investigation of the features of 2-D networks with $Al_2P_3O_{12}^{3-}$ stoichiometry, the following building rules are discovered: (i) the primary building unit in Figure

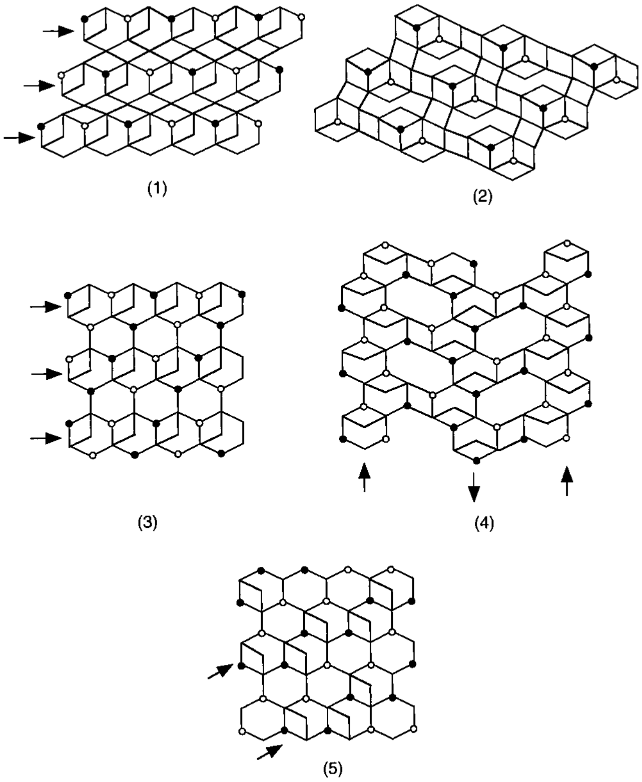
(1) (2) (3) (4) (5)

Figure 7. Geometries of known 2-D aluminophosphates with $Al_2P_3O_{12}^{3-}$stoichiometry (1) compound **1**, $[Al_2P_3O_{10}(OH)_2][C_6NH_8]$; (2) compound **2**, $Al_2P_3O_{12}H_2$·PyH; (3) compound **3**, $Al_2P_3O_{12}H$·$2C_5NH_{12}$ (UT-5); (4) compound **4**, $Al_2P_3O_{12}H$·$2C_5NH_{12}$ (UT-4); and (5) compound **5**, $Al_2P_3O_{12}H$·$2BuNH_3$. The black and white circles indicate the up and down features of triply bridging phosphate groups. The arrows show the edge-sharing bridged-6MR.

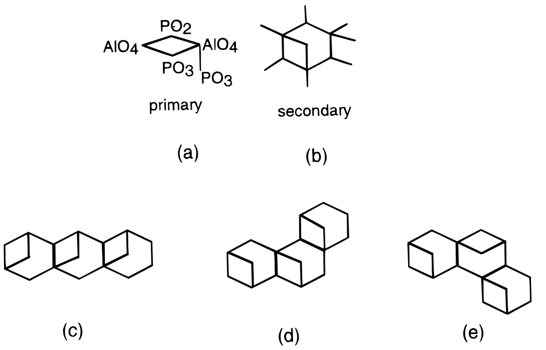

(a) (b) (c) (d) (e)

Figure 8. Primary and secondary building units (a and b); three modes of edge-sharing (c–e).

8a is typical for the stoichiometry of $Al_2P_3O_{12}^{3-}$; (ii) the bridged-6MR (Figure 8b) is commonly observed as a secondary building unit in these compounds; and (iii) to keep this stoichiometry, the bridged-6MR shares two edges of an hexagon as shown in Figure 8c,d. Furthermore, there is another possibility for sharing the edges of the hexagon (Figure 8e). Based on the above building rules, a large number of 2-D networks with the $Al_2P_3O_{12}^{3-}$ stoichiometry can be designed. Figure 9 presents several typical hypothetical 2-D networks with $Al_2P_3O_{12}^{3-}$ stoichiometry (the up and down feature shown in these structures is only one of the possibilities for each case).

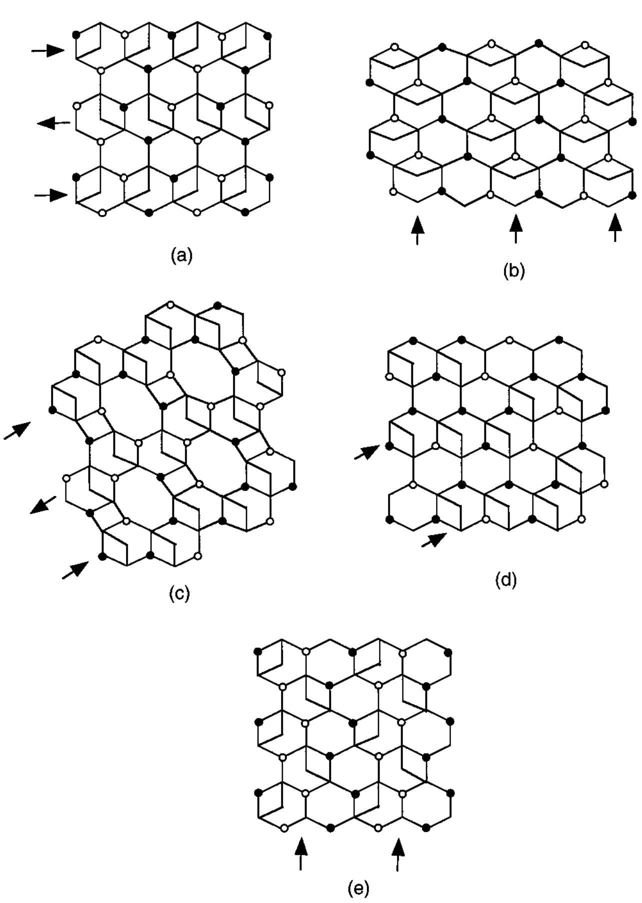
(a) (b) (c) (d) (e)

Figure 9. Hypothetical 2-D networks of aluminophosphates with $Al_2P_3O_{12}^{3-}$ stoichiometry.

It is well-known that the architectures of inorganic layers are greatly controlled by the organic templates (structure-directing agents). Cycloamines (with an exception of 2-$BuNH_2$, which gives compound **5**, $Al_2P_3O_{12}H$·$2BuNH_3$),[25] such as cyclohexylamine (for compounds **3** and **4**),[26] cyclopentylamine (for UT-3, isostructure with compound **3**),[27] pyridine (for compound **2**),[25] and 4-methylpyridine (compound **1**), are found to be favorable for the formation of $Al_2P_3O_{12}^{3-}$ stoichiometry. Further work is being focused on how to judiciously select the template agents for directing the hypothetical structures on the basis of analyzing the interlayer arrangement and the interaction between the templates and frameworks.

Conclusion

This work presents a new type of 2-D aluminophosphate $[Al_2P_3O_{10}(OH)_2][C_6NH_8]$ characterized by rows of edge-sharing bridged-6MRs and zigzag 4MRs. This new structure has potential for further setting up a 3-D framework through condensation of additional Al units across the hydrogen-bonding bridges between the two layers. On further investigation of the known 2-D aluminophosphates with $Al_2P_3O_{12}^{3-}$stoichiometry, some building rules have been first discussed, which allows the design of new 2-D networks. The synthesis of aluminophosphates with $Al_2P_3O_{12}^{3-}$ stoichiometry is suggested to be favored by use of alcohol as a solvent and cycloamine as a template. This work will promote the continuing synthesis of new materials with tailor-made structures and properties.

Acknowledgment. We are grateful to the CREST (Japan Science and Technology Corporation) for financial support.

Supporting Information Available: Complete tables of crystallographic conditions, atomic coordinates, anisotropic thermal parameters, bond lengths and angles, hydrogen coordinates, and isotropic displacement parameters (6 pages). Ordering information is given on any current masthead page.

CM980379C